Supporting Information

When the Signal is not from the Original Molecule to be Detected: Chemical Transformation of para-Aminothiophenol on Ag during the SERS Measurement

Yi-Fan Huang, Hong-Ping Zhu, Guo-Kun Liu, De-Yin Wu, Bin Ren* and Zhong-Qun Tian*

State Key Laboratory of Physical Chemistry of Solid Surfaces and Department of Chemistry, College of Chemistry and Chemical Engineering, Xiamen University, Xiamen 361005, China.

E-mail: bren@xmu.edu.cn; dywu@xmu.edu.cn

RECEIVED DATE (to be automatically inserted after your manuscript is accepted if required according to the journal that you are submitting your paper to)

S1. The roughening procedure for obtaining a SERS-active Ag electrode

An Ag disk electrode with a diameter of 2 mm was mechanically polished to mirror like. Then, it was immersed in an electrochemical cell containing 0.1 M KCl solution. The potential was first scanned from −0.2V to 0.6 V at a rate of 0.01 V/s, then stepped to −1.3 V, and finally scanned to −1.5 V at a rate of 0.001 V/s for a complete reduction. A saturated calomel electrode (SCE) was used as the reference electrode in all electrochemical and electrochemical-SERS (EC-SERS) experiments.

S2. The power dependent EC-SERS study of PATP on roughened Ag electrodes

A roughened Ag electrode was immersed in the 1 mM PATP ethanolic solution for 30 min. Then, the electrode was rinsed with ethanol and transferred into the spectroelectrochemical cell for cyclic voltammetric (CV) and EC-SERS experiments. 0.1 M $NaClO_4$ aqueous solution was used as the supporting electrolyte and was deaerated with the ultrapure nitrogen gas for 30 min before the CV experiment. The CV and EC-SERS experiments were performed in this solution.

Raman spectra were obtained using a confocal microprobe Raman instrument (LabRam I, Jobin-Yvon, France). The excitation line was 632.8 nm from a He-Ne laser. The objective was 50× with a numerical aperture of 0.55 and a working distance of 8 mm, resulting in a laser spot size of ca. 1~2 μm on the Ag surface. The experiments excited by a laser with a high power density were performed by directly focusing a laser with a power of 0.6 mW on the Ag surface. Therefore, the power density was ca. 2×10^7 mW/cm^2. In contrast, in order to achieve a very low power density but remain a good signal intensity, the laser was defocused for ca. 75 μm from the focal plane instead of simply decreasing the laser power, which resulting in a power density of ca. 8×10^2 mW/cm^2. The acquisition time for the high and low density experiments was 5 s and 90 s, respectively. Please refer to ref. 4d in the main text for detailed principle of the SERS defocusing technique.

S3. The surface mass spectroscopic (SMS) experiment of the PATP on the roughened silver

The roughened Ag electrode adsorbed with PATP (described in S1 and S2) was illuminated with a focused laser at a power of 0.6 mW (the same as that used in the SERS measurement at a high power density) randomly on the surface for tens of points. The SERS spectra of all the points were checked, which show the typical feature of DMAB. After that, the electrode was used for the SMS experiment directly. The controls, blank silver and silver adsorbed with PATP, were prepared according to S1 and S2, respectively, but without laser illumination.

The surface mass spectra were obtained using a Bruker Esquire HCT ion trap mass spectrometer (Billerica, MA, USA) coupled with a home-made desorption electrospray ionization (DESI) source.[RS1]

The HPLC grade methanol was used as the spray solvent. Bombarded by the solvent, the adsorbate was desorbed and drifted into the MS-inlet capillary for detection.

As shown in the Figure 2 in the main text, the mass spectra become very complicated due to the chemical ionization of the solvent as well as the surface species and the chemical activity of the Ag electrode. For example, the peak at ca. 218.0 can be easily ascribed to the Ag_2^+ cluster. Therefore, one may naturally argue that the species (DMAB) detected during the SMS may be produced during the ionization process of the adsorbed PATP, as the oxidation may also occur in the detection of mass spectroscopy.[RS2] To exclude this possibility, we did control experiments using the blank roughened silver electrode and the roughened silver electrode adsorbed with PATP, both of which have not been illuminated with laser. On both PATP adsorbed sample, we detected the peak which can be ascribed to PATP. But only on the sample that has been illuminated with laser, we detected the peak at 245.5 ascribed to DMAB related fragment (H+S-Ph-N=N-Ph-S). Therefore, SMS result convincingly points to the fact that DMAB was generated from PATP under the illumination of the high power laser.

S4. The synthesis of DMAB

The preparation of DMAB comprises the following steps: (1) aniline was dissolved in $NaHCO_3/H_2O$ solution and reacted with I_2 for 0.5 h to give 4-iodo-aniline, which was decolorized with $NaHSO_3$ and sublimed prior to use; (2) 4-iodo-aniline was then reacted with $NaBO_3 \bullet 4H_2O/H_3BO_3$ at 50~60 ^oC in an acetic acid medium for 6 h, affording orange-red crystals of 4,4'-diiodo-azobenzene after recrystallization in THF; (3) under dinitrogen atmosphere, 4,4'-diiodo-azobenzene was reacted with Mg in THF at 60 ^oC for 24 h. Sulfur was added, and the mixture was allowed upon heat treatment (60 ^oC) for 12-25 h. After workup, the mixture was quenched with saturated NH_4Cl/H_2O solution and then acidified with the HCl aqueous solution. By recrystallization, light yellow solids of DMAB were obtained. Detailed synthetic procedures were presented in the reference,[RS3] and related characterization data for DMAB were included here. M.p.: 127.8 ºC; ^{1}H NMR (400 MHz, $CDCl_3$, 298 K，ppm): δ 7.48 (d, $^3J_{HH}$ = 8.8 Hz, 4 H); 6.62 (d, $^3J_{HH}$ = 8.8 Hz, 4 H); 5.64 (s, 2 H); ^{13}C NMR (100 MHz, $CDCl_3$, 298

K，ppm): δ 148.1, 138.0, 114.5, 81.4; IR (Nujol mull, KBr, cm^{-1}): 2370, 1575, 1562, 1464, 1377, 1296, 1278, 1261, 1096, 1052, 1003, 834, 714; Anal. Calcd for $C_{12}H_{10}N_2S_2$ (M_r = 246.35), calcd: C 58.51, H 4.09, N 11.37; found: C 57.98, H 3.91, N 10.84.

In addition, the ^1H and ^{13}C NMR and IR spectra recorded are enhanced in Figures S1 and S2, respectively, for confirming the experimental achievement of DMAB as a stable compound. The SH functionality of DMAB was proved by a characteristic proton resonance at 5.64 ppm. The IR band at 2370 cm^{-1} corresponds to the S–H stretching frequency, and at 1377 cm^{-1} and 1464 cm^{-1} to the N=N one.

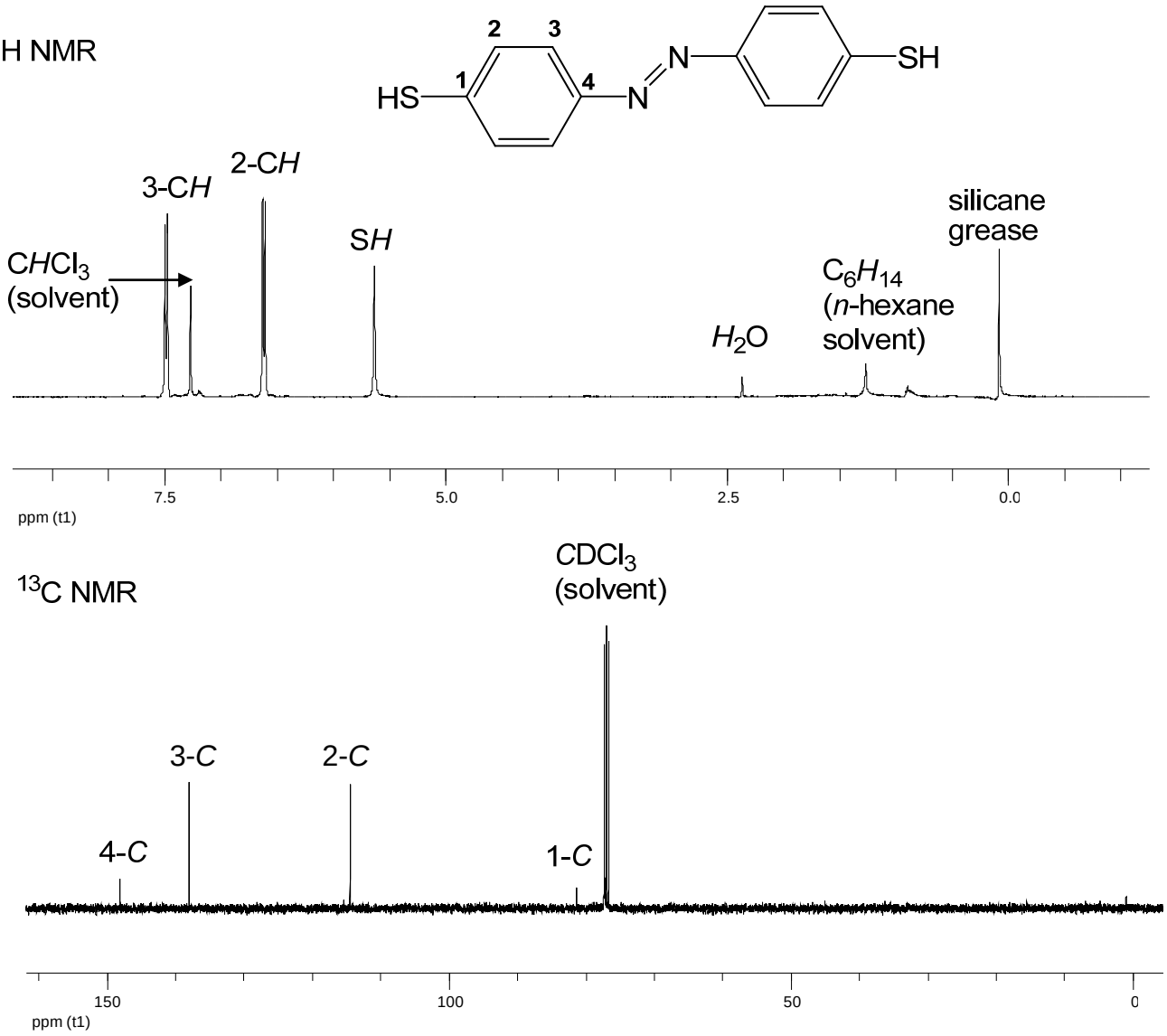

Figure S1. ^1H and ^{13}C NMR spectra of DMAB

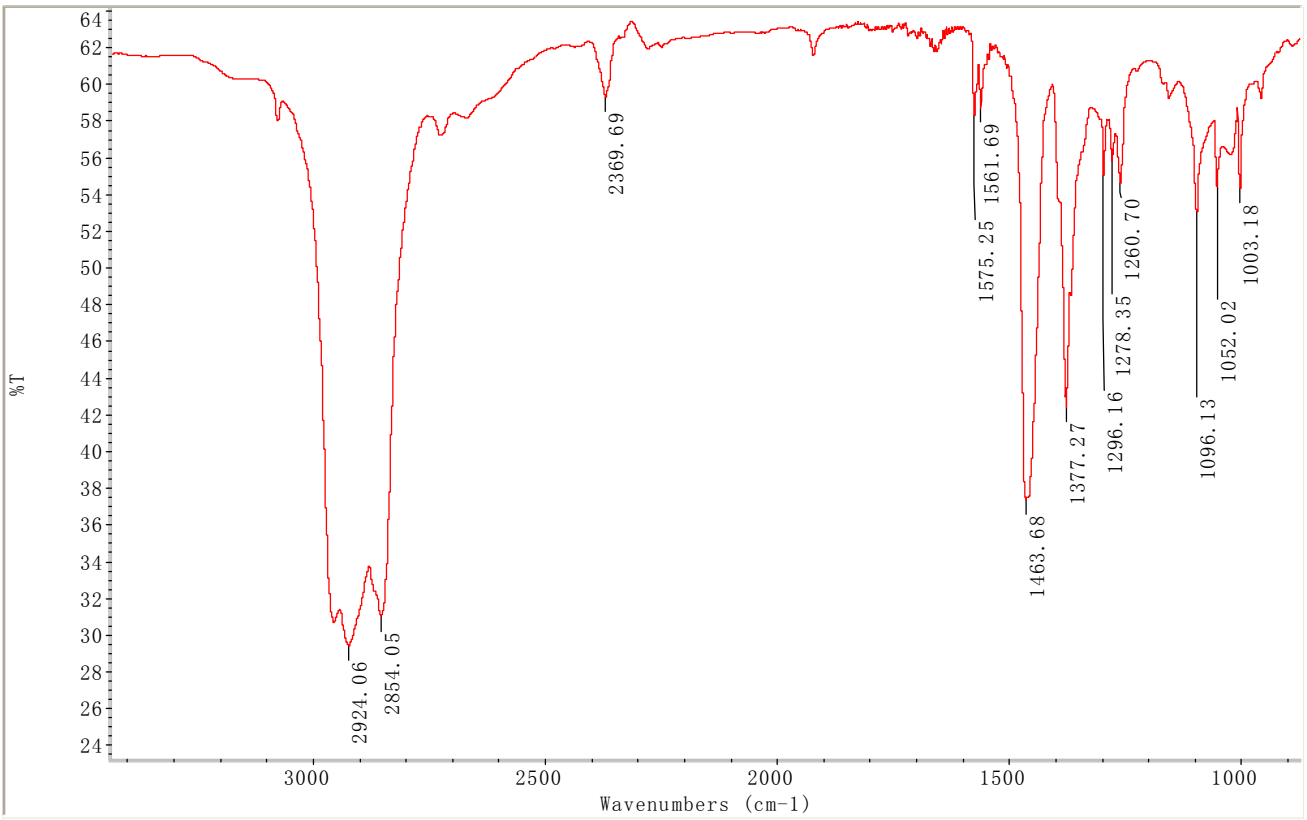

Figure S2. IR spectrum of DMAB

S5. The SERS experiment of PATP and DMAB on a roughened silver electrode

The SERS spectra of PATP and DMAB on the roughened silver electrode were both excited by a laser at a power density of 1×10^8 mW/cm^2.

According to the above SMS result, there were still some PATP on the surface. However, the SERS spectra of the two species as shown in Figure S3 present a very similar spectral feature. Our previous calculation has revealed that DMAB has about 100-folds larger Raman scattering cross-section than that of PATP, see ref.4c in the main text. Therefore, a minor amount of DMAB can give much stronger SERS signal than that of PATP with a much higher surface concentration.

In the SERS of PATP, the DMAB was produced by the oxidation of two adsorbed PATP. Therefore, there will be no S-H group in the final product. However, in the synthesized DMAB, one may expect to observe the Raman signal of a free S-H group if the molecule binds to the surface with one end. Interestingly, the missing signal of S-H was also observed in 1,4-benzenedithiol (BDT) by Kim's

group.[RS4, RS5] By systematically comparing the spectral feature of BDT on silver and gold, they proposed a flat lying configuration on the surface.[RS5] A same phenomenon may also occur in our system. Other reasons for not being able to observe the S-H signal may be due to that the 632.8 nm excitation is out of resonance of SPR of the Ag substrate and a lower detection sensitivity of the CCD detector at ~2500 cm^{-1}(at 750 nm).

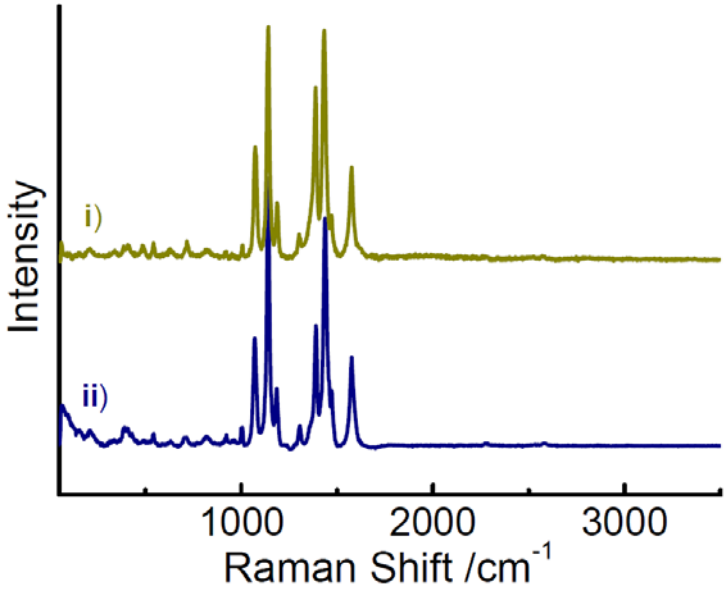

Figure S3. The SERS spectra of PATP (i) and DMAB (ii) on a roughened silver in air.

S6. Vibrational assignment of DMAB

In order to correlate the Raman and the SERS of DMAB, the Raman spectrum and the vibrational assignment on the basis of ref 4c in the main text were present in Figure S4 and Table S1.

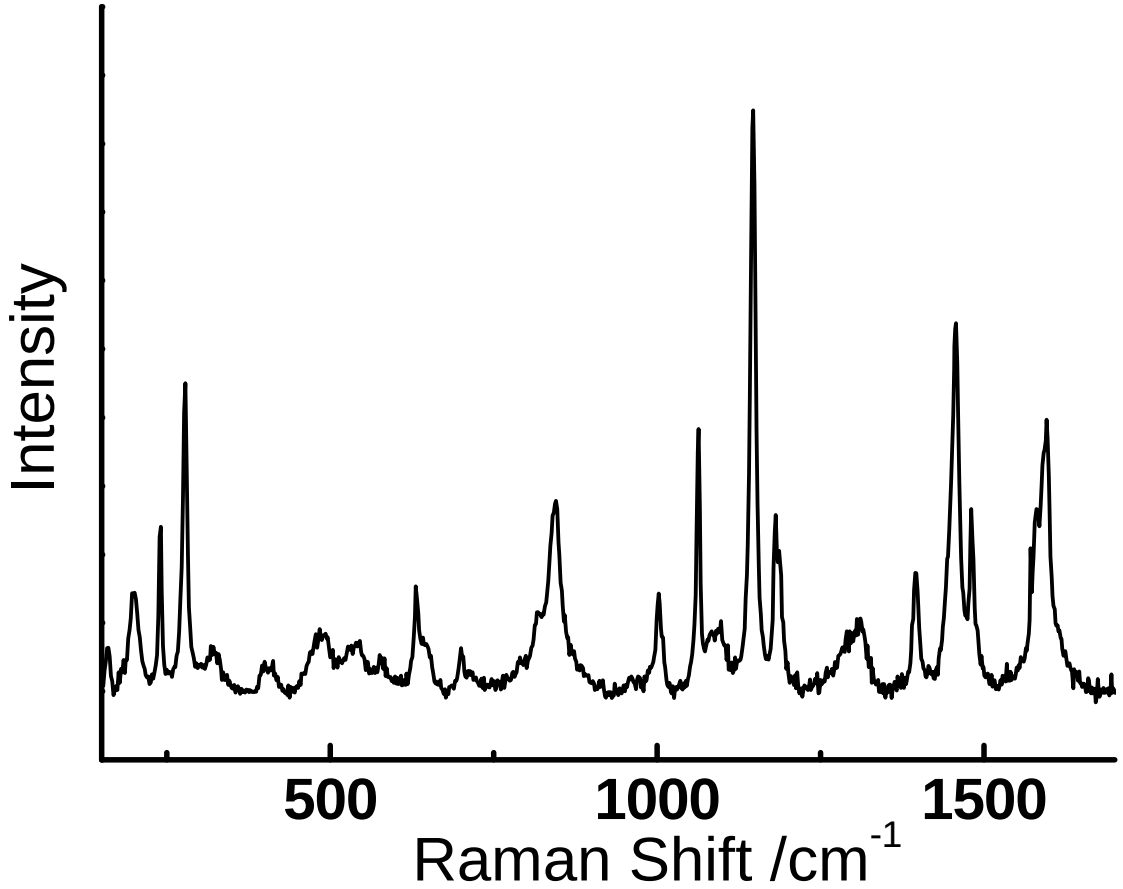

Figure S4. The Raman Spectrum of DMAB

Table S1. Experimental and theoretical vibrational frequencies (cm^{-1}), potential energy distribution (PED), assignments of DMAB calculated at the level of PW91PW91/6-311+G**. The PED values are listed in the parenthesis of the corresponding internal coordinates.

Experimental			Theory		Assignments
IR	Solid	SERS	DMAB	Ag_5-DMAB-Ag_5	
			2614.1		$\upsilon_{SH(100)}$
			2614.1		$\upsilon_{SH(100)}$
	1588	1576	1590.4	1583.5	$\upsilon_{CC(54)}$ (ν_{8a})
1575.3			1586.0	1578.6	$\upsilon_{CC(58)}$ (ν_{8a})

			1555.1	1548.2	$\upsilon_{CC(61)}$ (ν_{8b})
1561.7			1549.4	1541.5	$\upsilon_{CC(70)}$ (ν_{8b})
	1481	1472	1466.2	1459.4	$\beta_{C\text{-}H(46)}+\upsilon_{NN(19)}+\upsilon_{CC(12)}$ (ν_{19a})
1463.7			1465.1	1457.9	$\beta_{C\text{-}H(56)}+\upsilon_{CC(24)}$ (ν_{19a})
	1456	1438	1429.1	1423.8	$\upsilon_{NN(31)}+\upsilon_{CC(23)}+\beta_{C\text{-}H(25)}$
1377.3			1410.2	1401.5	$\upsilon_{CC(72)}+\beta_{C\text{-}H(34)}$ (ν_{19b})
	1395	1389	1393.2	1386.8	$\upsilon_{NN(44)}+\upsilon_{CC(30)}+\beta_{C\text{-}H(24)}$
			1336.6	1326.2	$\upsilon_{CC(100)}$ (ν_{15})
	1306	1305	1331.5	1320.4	$\upsilon_{CC(100)}$ (ν_{15})
			1280.4	1270.1	$\beta_{C\text{-}H(83)}$ (ν_{14})
			1277.4	1268.1	$\beta_{C\text{-}H(81)}$ (ν_{14})
1260.7			1242.9	1238.8	$\upsilon_{CN(51)}+\upsilon_{CC(15)}+\beta_{C\text{-}H(18)}$
	1183	1187	1192.2	1187.3	$\upsilon_{CN(35)}+\beta_{C\text{-}H(32)}+\upsilon_{CC(17)}$
			1141.1	1138.1	$\beta_{C\text{-}H(68)}+\upsilon_{CN(10)}$
	1147	1141	1129.2	1126.8	$\beta_{C\text{-}H(45)}+\upsilon_{CN(35)}$
			1099.3	1089.9	$\beta_{C\text{-}H(63)}+\upsilon_{CC(14)}$ (ν_{18a})
1089.9			1095.9	1086.4	$\beta_{C\text{-}H(58)}+\upsilon_{CC(14)}$ (ν_{18a})
	1064	1074	1082.9	1064.7	$\upsilon_{CC(40)}+\upsilon_{CS(28)}$ (ν_1)
1063.6			1082.1	1063.6	$\upsilon_{CC(42)}+\upsilon_{CS(29)}$ (ν_1)
	1002	1004	992.7	991.1	$\alpha_{CCC(49)}+\upsilon_{CC(22)}$ (ν_{12})
1003.2			992.3	990.8	$\alpha_{CCC(50)}+\upsilon_{CC(22)}$ (ν_{12})

υ, α, and β denote the stretching coordinate, ring bending coordinate, and the in-plane bending coordinate out of the benzene ring, respectively. Wilson symbols for the vibrational modes in two phenyl rings in DMAB are presented in the parenthesis of the last column. Some modes involving the coupling between the ring coordinates and the C-N stretch/the N-N stretch are not labeled.

REFERENCES

(RS1) Xie Y.; He L.F.; Lin S.C.; Su H.F.; Xie S.Y.; Huang R.B.; Zheng L.S. *J. Am. Soc. Mass. Spectrom.* **2009**, *20*, 2087-2092.

(RS2) Pitteri, S. J.; McLuckey, S. A. *Mass Spectrom. Rev.* **2005**, *24*, 931.

(RS3) Zhu, H.P.; Zheng, Z.Y.; Wang, J.J.; Ren, B.; Huang, Y.F.; Wu, D.Y. 4,4'-Dimercaptoazobenzene and its Preparation. Chinese Patent, 2009 in pending.

(RS4) Cho, S. H.; Han, H. S.; Jang, D. J.; Kim, K.; Kim, M. S. *J. Phys. Chem.* **1995**, *99*, 10594.

(RS5) Joo, S. W.; Han, S. W.; Kim, K. *J. Colloid Interf. Sci.* **2001**, *240*, 391.